Determination of Atomic Positions in a Solid Xe Precipitate Embedded in an Al Matrix

K. Mitsuishi

National Research Institute for Metals, Sakura, Tsukuba 305, Japan

M. Kawasaki

JEOL Ltd., Akishima, Tokyo 196, Japan

M. Takeguchi and K. Furuya

National Research Institute for Metals, Sakura, Tsukuba 305, Japan
(Received 9 November 1998)

The atomic structure of precipitates embedded in crystalline membranes was observed for the first time by high-angle annular dark field scanning transmission electron microscopy (HAADF-STEM) with an electron probe in an atomic dimension. The experimental image was analyzed by taking a line profile and was compared with the calculated intensities obtained from the multislice based HAADF-STEM simulation. A model shifting Xe atoms slightly from the on-site of the Al matrix in the [100] direction agreed well with the experimental profile and image. From these results, the small displacement of Xe atoms to the Al matrix is estimated at about 0.5 Å. [S0031-9007(99)08889-4]

The behavior of nanometer-size precipitates created by implantation of inert gases in materials has been studied extensively for more than 35 years because of problems associated with the development of fusion and fission reactors [1,2]. Up to date, it has been discovered that the rare gas Xe forms solid nanocrystals of less than 4 nm radius and is mesotactically aligned with the surrounding matrix when it is implanted at room temperature. The shape and topotactical alignment of the precipitates have been investigated by high-resolution transmission electron microscopy (HRTEM) [3–5]. It is fully accepted that the Xe precipitate has the shape of a cubeoctahedron with an fcc structure consisting of eight {111} planes and six {100} planes having a 50% larger lattice constant to the Al matrix. However, the positional relationship between Al and Xe has not been clarified because the HRTEM image is a phase contrast image and is not so sensitive to slight positional displacement.

Since the image of isolated heavy atoms was obtained using a scanning transmission electron microscope (STEM) equipped with annular detector [6], a method has been developed at a constant pace to improve the point-to-point resolution that has now reached 0.13 nm [7]. By using a high-angle, wide-angular-range annular detector, the image is shown to mainly consist of thermal diffuse scattering electrons, and the coherent contribution of the image is averaged to be the incoherent image with a strong Z contrast [8–11]. Therefore, the images obtained from the high-angle annular dark field scanning transmission electron microscopy (HAADF-STEM) method can be intuitively interpreted with no contrast reversals along with the defocus and/or specimen thickness changes, in contrast to the phase contrast images from HRTEM. Furthermore, HAADF-STEM with electron probes in an atomic dimension can be expected to be a position sensitive method when used for the observation of precipitates.

In this paper, HAADF-STEM observation of precipitates embedded in crystalline membranes was made for the first time with electron probes of atomic dimension. Solid Xe precipitate in the Al matrix was chosen because of the large difference in the electron scattering factors of Al and Xe. The images obtained were analyzed by taking a line profile and were compared with the calculated intensities obtained by the multislice based HAADF-STEM simulation.

Experimental.—The Al specimens were cut from 5N starting material and electronically polished so as to be TEM specimens. The Xe precipitates embedded in Al were made by the implantation of 30 keV Xe at room temperature to a dose of 3×10^{19} ions/m^2. Specimens were then annealed at 523 K for 0.5 h in a vacuum to remove residual radiation damage in the Al matrix and to consolidate the Xe within the precipitates.

HAADF-STEM was performed with a JEM-2010F-STEM, operated at 200 kV. The spherical aberration Cs and the aberration angle of the probe forming lens are 1.0 mm and 10 mrad, respectively. The defocus value was taken as −50.1 nm, which corresponds to the Scherzer focus of a 0.15 nm probe size. The angular range of the annular dark field detector was set from 50 to 100 mrad. The observation was performed at room temperature.

Multislice [12] programs included in the EMS program package of P. A. Stadelmann [13] were modified to simulate the HAADF-STEM image intensities. Modification was made using Nakamura's method [14] expressing the distribution of thermal diffuse scattering electrons as a Gaussian function. Weickenmeier's absorptive scattering factor [15] was used as in the EMS programs. A

Debye-Waller factor of 0.005 nm² was used for both Xe and Al atoms.

Xe precipitates in an Al lattice were modeled as a cubeoctahedron with faces parallel to [111] and [100] in the Al cavities, which was faceted on these crystal planes [16,17]. The lattice parameter of the fcc Xe crystal was chosen to be 50% larger than that of Al, consistent with electron diffraction data. The relaxation of interface atoms was not included. The potential used in the calculation was made from 117 of Xe atoms of precipitate embedded in the center of 30 layers of Al lattice.

Results and discussion.—Based on HRTEM observations [3–5], the relationship between Xe and Al lattices has been reported as a cube-cube orientation with parallel close-packed planes and directions: $(111)_{Al} \parallel (111)_{Xe}$ and $[110]_{Al} \parallel [110]_{Xe}$. When observations were made along low index orientations such as [011] and [111], two configurations of the Xe-Al relation were drawn, namely, a perfect overlap of Xe and Al atoms, and a Xe atom located between two Al atoms. Figure 1 shows a HAADF-STEM image of Xe precipitate in Al along the [011] direction (a) before and (b) after the image processing by Fourier filtering. The mask of 2.5 nm⁻¹ diameter is applied to the center spot and to each of the nearest six spots of Xe and Al. In Fig. 1(b), Moiré-like patterns were observed in the same manner as with HRTEM [3–5]. It is important to point out that the pattern is asymmetric in this image. The pattern mainly consists of two trianglelike patterns. One is a large triangle with sides of three atoms spacing of Al, and the other is a small triangle made up of three atoms. The white arrow in the figure goes across these triangles from the vertex of the large one to that of the small one. It is speculated that these patterns are caused by the slight displacement of Xe atoms from the Al lattice point on which the Xe atoms appear according to the HRTEM observations. Since the patterns are observed in the whole area of the nanocrystal, the displacement is symmetrical toward the Al lattice points.

To clarify these matters in more detail, intensity profiles of atoms along the white arrow in Fig. 1 were measured and shown in Fig. 2. The solid line indicates the experimental data. The two others are calculated intensities by modified multislice simulation. The dashed line was obtained by using a model of the Xe atoms for HRTEM, in which a cube-cube orientation between Al and Xe was adopted with perfect overlap of two lattices. The dotted line was obtained by another model, in which a small displacement of Xe atoms against Al lattice points was introduced. The displacement is about 0.5 Å in the [100] direction and also keeps a symmetrical positional relationship between Xe and Al. The intensities of these profiles were normalized in such a way that the areas under each line became constant. In the experimental curve, there are large and small peaks corresponding to the vertex and base of the large triangle, respectively. A blurred peak with a medium height corresponds to the small triangle. As for the dashed line with the non-atom-shift model, a sharp peak was observed where the Xe and Al atoms overlapped each other. The peak position is a little to the left compared to the experimental one, and neither the peak width nor the height coincides well with the experimental ones. The other three medium peaks with almost the same shape and height as each other also disagreed with the experimental ones. On the other hand, as for the dotted line with the atom-shift model, the height of the large peak decreases and the position is slightly shifted to the right, showing good agreement with the experimental one. The peaks, corresponding to the small triangle, are connected to each other, forming one blurred peak as seen in the experimental ones. The shape of the small peak in the large triangle was not well reproduced even in the simulation with the atom-shift model. This may be due to the size of the Xe precipitate used in the calculation,
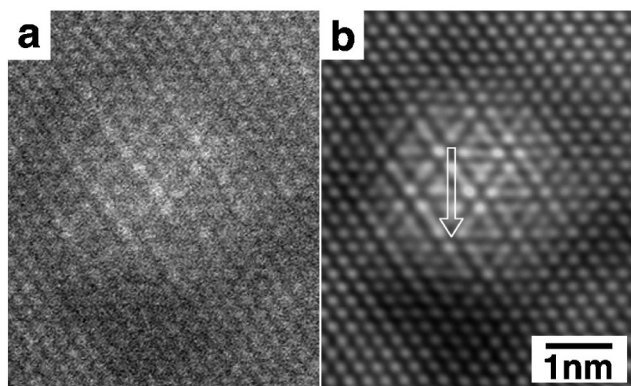

FIG. 1. Experimental HAADF observation results of the Xe precipitate in Al (a) before and (b) after image processing by Fourier filtering, respectively. The large and small trianglelike patterns were observed in the figure after filtering.
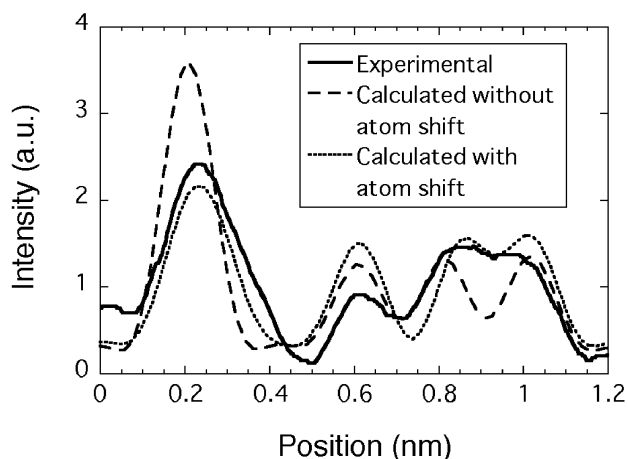

FIG. 2. Intensity profiles along the white arrow in Fig. 1. The solid line indicates the intensity obtained from the experiment, the dashed line shows the calculated intensities using the model of Xe atoms when exactly on the Al lattice point, and the dotted line is for the model introducing the displacement of Xe atoms to the Al lattice point.
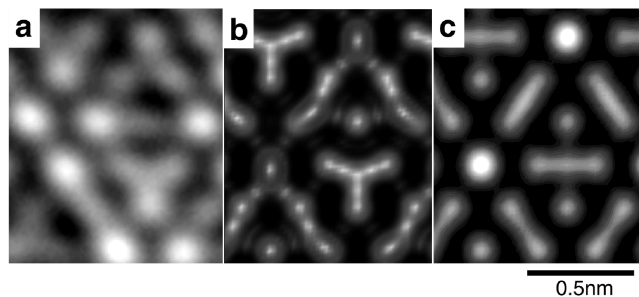
0.5nm

FIG. 3. The central part of the image. (a) The experimental image. (b) The corresponding region of the simulated image using the shifted model. (c) The calculated image using the no-atom-shift model.

which is smaller than the experimental one. The thickness of the Al layers and depth of the precipitate also had some influence on these intensity relationships. For more accurate results, the optimization of these values by recursive calculations would be required.

The central part of the precipitate is shown in Fig. 3 where (a) is the experimental image and (b) and (c) are the calculated images of corresponding regions of the precipitate using the models used in Fig. 2, with and without the atom shift, respectively. The large and small trianglelike patterns in the experiment are well reproduced in Fig. 3(b) indicating that the small displacement of the Xe atoms toward Al coincided well with the experimental ones.

In conclusion, HAADF-STEM observation of precipitates embedded in crystalline membranes was made for the first time using electron probes of atomic dimensions. The HAADF-STEM images of Xe precipitates embedded in Al were not similar to those from the results of an HRTEM. Multislice based HAADF-STEM simulation was made for these images taking into account the distribution of thermal diffuse scattering as a Gaussian function. Although the precipitates were considered to have a three-dimensional structure with a cube-cube orientation relationship with the Al matrix, calculated intensities did not coincide well with the experimental images when a perfect overlap between Al and Xe lattices was assumed.

Fitting of simulated image intensities to experimental images was carried out with a model introducing a slight displacement of the Xe atoms in the [110] plane. The amount and direction of the displacement were 0.5 Å and [100], respectively. From these results, it can be said that the Xe atoms are shifted from the Al lattice points.

Quantitative agreement, however, would require recursive calculations to optimize parameters of precipitate size, thickness of Al layers, and depth of precipitate, because not only the HAADF-STEM intensity of Xe atoms itself, but also the visibility of atoms shifted from Al atom columns, largely depends on these parameters.

The displacement only in [110] explains the experimental image well. This fact indicates that a definite crystallographic orientation relationship exists between the two lattices. Further experiment and analysis will be required to discuss the universality of the displacement and dependence regarding the precipitate size.

[1] S. Furuno, K. Hojou, K. Izui, and T. Kino, J. Nucl. Mater. **155–157**, 1149 (1988).
[2] V. N. Chernikov, W. Kesternich, and H. Ullmaire, J. Nucl. Mater. **227**, 157 (1996).
[3] S. E. Donnelly and C. J. Rossouw, Phys. Rev. B **13**, 485 (1986).
[4] D. I. Potter and C. J. Rossouw, J. Nucl. Mater. **161**, 124 (1989).
[5] S. E. Donnelly and J. Rossouw, Science **230**, 1272 (1985).
[6] A. V. Crewe, J. P. Langmore, and M. S. Isaacson, *Physical Aspects of Electron Microscopy and Microbeam Analysis,* edited by B. M. Siegel and D. K. Beaman (Wiley, New York, 1975), pp. 47–62.
[7] H. S. von Harrach, Ultramicroscopy **58**, 1–5 (1995).
[8] S. J. Pennycook and D. E. Jesson, Phys. Rev. Lett. **64**, 938–941 (1990).
[9] S. J. Pennycook, D. E. Jesson, A. J. McGibbon, and P. D. Nellist, J. Electron. Microsc. **45**, 26–43 (1996).
[10] Z. L. Wang and J. M. Cowley, Ultramicroscopy **31**, 437–454 (1989).
[11] Z. L. Wang and J. M. Cowley, Ultramicroscopy **32**, 275-289 (1990).
[12] K. Ishizuka, Acta Crystallogr. Sec. A **38**, 773–779 (1982).
[13] P. A. Stadelmann, Ultramicroscopy **21**, 131–146 (1987).
[14] K. Nakamura, H. Kakibayashi, K. Kanehori, and N. Tanaka, J. Electron. Microsc. **1**, 33–43 (1997).
[15] A. Weickenmeier and H. Kohl, Acta Crystallogr. Sec. A **47**, 590–597 (1991).
[16] L. Gråbæk, J. Bohr, H. H. Andersen, A. Johansen, E. Johnson, L. Sarholt-Kristensen, and I. K. Robinson, Phys. Rev. B **45**, 2628 (1992).
[17] S. Q. Xiao, E. Johnson, S. Hindenberger, A. Johannsen, K. K. Bourdelle, and U. Dahmen, J. Microsc. **180**, 61 (1995).